Climate Dynamics (1997) 13 : 733–744

Climate Dynamics

Modelling the short-term response of the Greenland ice-sheet to global warming

R. S. W. van de Wal, J. Oerlemans

Institute for Marine and Atmospheric Research, Utrecht University, Princetonplein 5, 3584 CC Utrecht, The Netherlands

Received: 21 August 1996/Accepted: 12 May 1997

Abstract. A two-dimensional vertically integrated ice flow model has been developed to test the importance of various processes and concepts used for the prediction of the contribution of the Greenland ice-sheet to sea-level rise over the next 350 y (short-term response). The mass balance is modelled by the degree-day method and the energy-balance method. The lithosphere is considered to respond isostatically to a point load and the time evolution of the bedrock follows from a viscous asthenosphere. According to the IPCC-IS92a scenario (with constant aerosols after 1990) the Greenland ice-sheet is likely to cause a global sea level rise of 10.4 cm by 2100 AD. It is shown, however, that the result is sensitive to precise model formulations and that simplifications as used in the sea-level projection in the IPCC-96 report yield less accurate results. Our model results indicate that, on a time scale of a hundred years, including the dynamic response of the ice-sheet yields more mass loss than the fixed response in which changes in geometry are not incorporated. It appears to be important to consider sliding, as well as the fact that climate sensitivity increases for larger perturbations. Variations in predicted sea-level change on a time scale of hundred years depend mostly on the initial state of the ice-sheet. On a time scale of a few hundred years, however, the variability in the predicted melt is dominated by the variability in the climate scenarios.

1 Introduction

Enhanced greenhouse warming will significantly affect the mass balance of ice-sheets and glaciers and will therefore change their size and shape. It is generally believed that in the next century glaciers and small ice caps will contribute more significantly to changes in ocean volume than the Greenland and Antarctic ice-sheets (Robin 1986; Oerlemans 1989; Warrick and Oerlemans 1990). In the 1990 IPCC sea-level projections, a fixed-geometry approach was used to calculate the contributions from Greenland and Antarctica, i.e. changes in ice-sheet geometry were not considered. In the light of results obtained with dynamic ice-sheet models (Oerlemans 1982; Huybrechts and Oerlemans 1990; Huybrechts et al. 1991), a reconsideration of that approach seems justified. Calculations with three-dimensional dynamic ice-sheet models, in spite of all their simplifications and problems with boundary conditions, indicate that the fixed geometry approach is valid only for periods shorter than about 60 y.

A few model studies have presented estimates of the response of the Greenland ice-sheet to climate change, (e.g. Huybrechts et al. 1991: Van de Wal and Oerlemans 1994). These estimates are difficult to compare, because different model formulations were employed. Huybrechts et al. (1991) used a degree-day model as mass balance forcing for their three-dimensional thermodynamical ice-sheet model, whereas Van de Wal and Oerlemans (1994) used an energy balance model but neglected variations in the geometry. Van de Wal (1996) compared a degree-day model and an energy balance model of the Greenland ice-sheet using a fixed geometry approach.

In this study we concentrate on the importance of various physical processes for the short-term response of the Greenland ice-sheet. For this purpose, we have developed a two-dimensional ice-sheet model which allows two formulations for the mass balance, and which includes ice dynamics and bedrock response. This model has been used to test the importance of various processes and concepts for the dynamic response of the Greenland ice-sheet on a time scale of a few hundred years. After discussing sensitivity experiments, we present several climate-change experiments using scenarios from the latest Kattenberg et al. (1996).

2 General concept of the model

In this section we give an overview of the model formulation. A more detailed description, with references, is presented in the Appendix. The model consists of three

Correspondence to: R. S. W. van de Wal
Fax: 31302543163
E-mail:wal@fys.ruu.nl

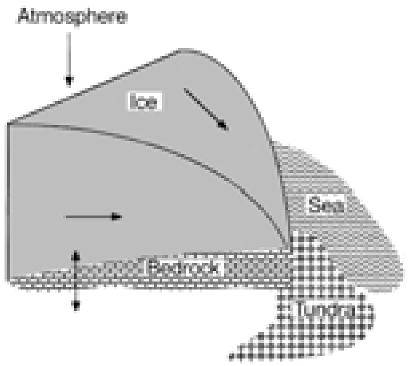

Fig. 1. The general concept of the model, illustrating the three "spheres": bedrock, ice and atmosphere. The model is two-dimensional in the horizontal (N—S and E—W). Calving is not explicitly calculated

components describing the solid earth, the ice-sheet and the interaction of ice surface and atmosphere (Fig. 1). The solid earth model is simply divided into a lithosphere and a viscous asthenosphere. The viscosity of the asthenosphere determines the time-dependent response of the bedrock. The lithosphere is considered to response isostatic to a point load. The difference in density of rock and ice drives the deformation of the earth's crust.

The ice-sheet model is two-dimensional, considering vertically integrated flow. Two different model versions are used: one including sliding and one excluding sliding. The model is tuned by adjusting flow parameters for ice deformation and sliding.

The third component represents the interaction of ice surface and atmosphere, which generates the mass balance (the driving force). We use two models. The first describes the mass balance as a function of the temperature alone, following the degree-day concept. This model is identical to the one described in Huybrechts et al. (1991). In the second model the mass balance is calculated with an energy balance method. Here the amount of energy available for melting is based on a calculation of the radiation budget and turbulent heat transfer between atmosphere and surface. Refreezing is parametrized in a simple way. Conduction in the surface layer is neglected. Cloudiness is parametrized according to the sparse measurements available and independent of the climate state considered. In effect this means that climate-change experiments involve changes in temperature and precipitation only. It should be noted that the effect of temperature changes is threefold: the longwave balance and the turbulent transfer both change, and the amount of refreezing meltwater in early summer is modified. More details on the energy balance model are provided in the Appendix and in Van de Wal and Oerlemans (1994).

The three model components are fully coupled. The mass balance is, for instance, determined by surface elevation. Surface elevation is influenced by ice flow and bedrock movements. Equilibrium states are therefore dependent on the formulation of all three model components. So, for instance, changing the mass-balance model from an energy balance method to a degree-day method will result in a different equilibrium state for the ice-sheet.

3 The reference experiment

Before climate change experiments are performed an equilibrium state has to be modelled for reference. It seems natural to consider a reference state which resembles the present state as closely as possible, even though this state may not be in equilibrium at all. It is difficult to analyze the reference state in the light of our rather limited knowledge about the present state. Consequently, various equilibrium states can be modelled which are all within the error limits of the observations, but may differ considerably at specific sites. Van de Wal and Ekholm (1996) show that the elevation distribution used by Huybrechts et al. (1991) and Van de Wal and Oerlemans (1994) led to a 20% overestimation of the present-day ablation in an energy-balance model as well as in a degree-day model. Here, we choose a reference state which is based on the physically most complete model for short-term response. In our opinion, such a model should contain bedrock response, ice sliding, and an energy-balance model to generate the mass-balance field. However, reasonably steady-states can also be achieved by all possible combinations of model components sliding/no-sliding; and degree-day/energy balance. In Fig. 2 and Tables 1 and 2 the reference state is analyzed.

In the model presented, the volume of the ice-sheet is about 3.5% smaller than derived from the digitised data set presented by Letréguilly et al. (1991), whereas the surface area is 3.5% larger (see Table 1). For comparison, Huybrechts et al. (1991) calculated a reference volume with a three-dimensional thermodynamical model which was 13% larger than deduced from the observations. General agreement between the two-dimensional model calculations and the observed elevation field can be seen in Fig. 2a, b. Here surface elevation from Ekholm (1996), projected on the 20*20 km grid, is used as observed surface elevation. The main features, the two-dome structure with the saddle in between and the steep eastern side of the ice-sheet are reproduced reasonably well by the model. Another encouraging aspect, important for ablation calculations, is that the area-elevation distribution is represented well by the model. On closer inspection, however, by looking at a difference map, large discrepancies are revealed locally (see Fig. 2c). Differences of more than 300 m occur over a total surface areas of $60 \cdot 10^3$ km^2 (roughly 3% of the total surface area). These points are more or less randomly distributed along the margin of the ice-sheets in clusters smaller than $4 \cdot 10^3$ km^2. The southern part of the modelled ice-sheet tends to be too low, whereas the south-western part shows isolated areas where the modelled elevations are too high. The agreement is generally better in the north.

Table 2 contains values for the mean elevation of the ice-sheet of the reference experiment and for the two elevation models. Surface elevation of the ice-sheet has been computed from data obtained by radio-echo sounding flights. These measurements were undertaken in the late 1970s by the Electromagnetic Institute of the Technical University of Denmark. Their measurements are referred to as the TUD-model, which was presented in digitized form by Letréguilly et al. (1991). The second present-day elevation distribution is based upon satellite

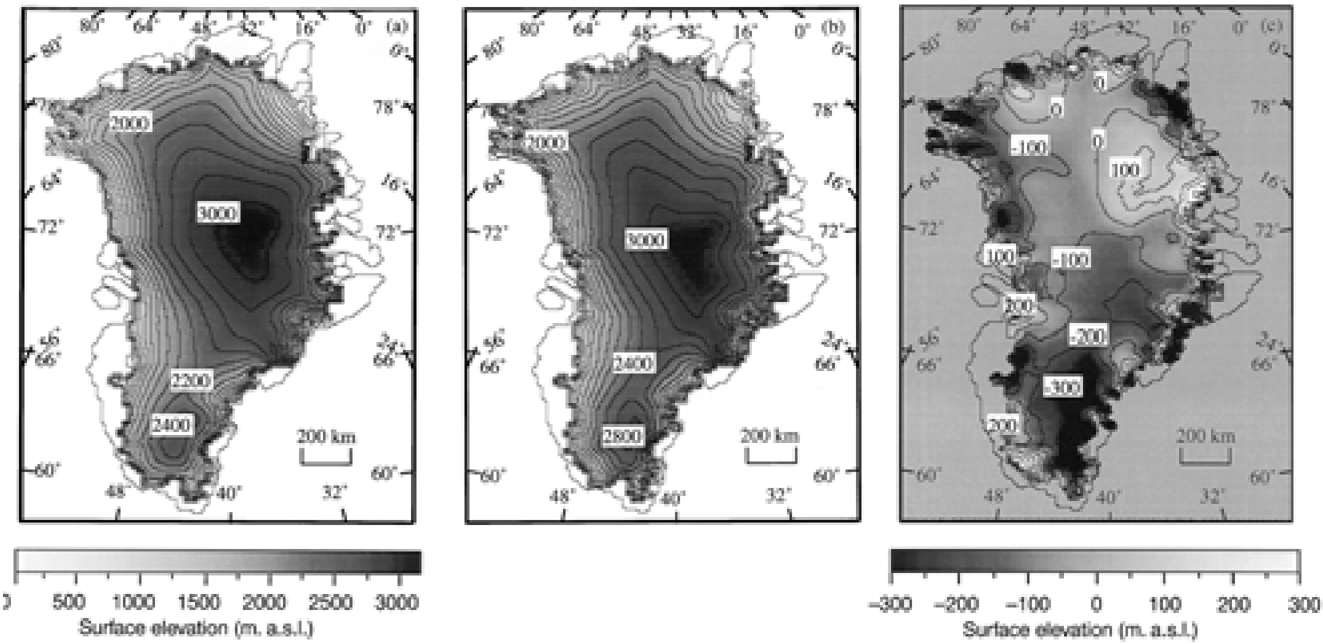

Fig. 2. Surface elevation for the reference experiment, **b** observations of the surface elevation derived from Ekholm et al. 1996, **c** and the difference between the reference experiment and the observations

Table 1. Volume and surface area of the Greenland ice-sheet

	Volume (10^6 km^3)	Surface area (10^6 km^2)	Remark
Reference experiment	2.73	1.73	2D ice sheet model
Letréguilly et al. 1991	2.83	1.67	from observations
Huybrechts et al. 1991	3.21	1.78	3D ice sheet model

Table 2. Mean elevation of the Greenland ice-sheet. The last column shows the mean elevation divided by the mean elevation of the IA-model. See text for explanation of the abbreviations IA and TUD

	Mean elevation (h_s) in m	h_s/h_s-IA
Referece experiment	2074	96%
IA-model	2159	100%
TUD-model	2126	98%

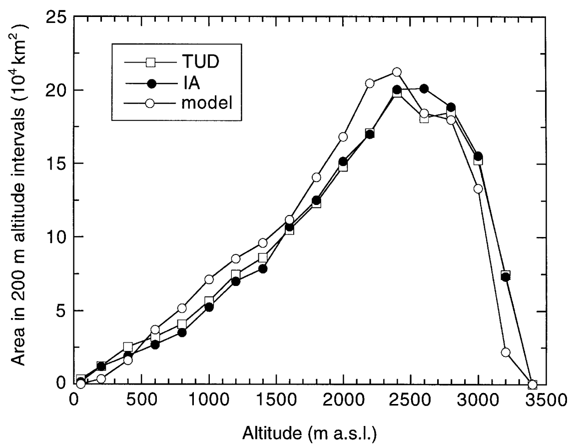

Fig. 3. Area-elevation distribution for the simulated ice sheet (reference experiment) and the two sets of observations (*IA* and *TUD*, see text)

altimetry data from GEOSAT and ERS-1 together with airborne laser altimetry, and local terrestrial surveys at the Summit. These data are referred to as the IA-model (Ekholm 1996). As can be seen in Table 2, the reference experiment has a slightly lower mean surface elevation than the two other models.

An alternative approach to compare model and observations is to consider the hypsometry. Figure 3 presents the hypsometric curves for the two observation fields (IA and TUD) and the modelled reference experiment. A close look at Fig. 3 shows that the difference between model and observation is largest between 2000 and 2500 m a.s.l. This results in a lower median for the model compared to the observations. Note that the two observation fields vary slightly in the lower areas below 1500 m a.s.l. and that the model follows the TUD- observational field better in this part of the hypsometric curve. Therefore we conclude that the ablation area, which is most important for the short term response of the ice-sheet, is captured reasonably well by the model. It must be realised that there is a considerable uncertainty in the observations (TUD-IA) (Van de Wal and Ekholm 1996) and the non-equilibrium state of the ice-sheet (e.g. Huybrechts 1994). The reference experiment presented in this section will therefore be used as a starting point for our perturbation experiments.

4 Climate scenarios

The IS92 radiative forcing scenarios (Kattenberg et al. 1996) were used to calculate the temperature perturbations needed as input for the climate change experiments with the Greenland ice-sheet model. These temperature perturbations were calculated with a two-dimensional energy balance climate model, having latitudinal and seasonal resolution (De Wolde et al. 1995). This model has a prescribed ocean circulation and the atmosphere is represented by a vertically and zonally averaged layer of air. The climate model has no explicit atmospheric dynamics, and the temperature perturbation over the Greenland ice-sheet is taken simply as the zonally-averaged temperature perturbations for the relevant latitude belts.

The various temperature scenarios used in this work are presented in Fig. 4 and 5. For the latitude belt 65–70 °N, Fig. 4 shows annual mean temperature change dependent on time. Compared to the calculated global mean temperature perturbation, (not shown) the values over Greenland are about 50% larger. This reflects the pole ward amplification of the temperature change due to snow and sea-ice feedback.

The temperature change is not uniform through the year. Figure 5 shows the seasonal variation for the IS92a scenario excluding aerosols (further referred to as AN) and for the IS92a scenario including aerosols (AF). The temperature changes are for 2100 relative to 1990. The predicted values are smallest for the summer and early fall, in accordance with most other model studies. It is noteworthy that the changes in winter temperature vary significantly with latitude.

The IPCC emission scenarios are given until 2100. As longer integrations with the ice-sheet model are carried out here, we have simply held all temperature perturbations equal to the 2100 values.

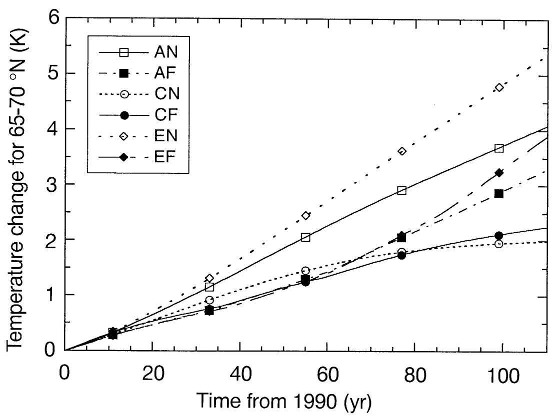

Fig. 4. Climate change scenarios used in this study. Here annual mean temperature perturbation for the 65–70 °N latitude belt is shown

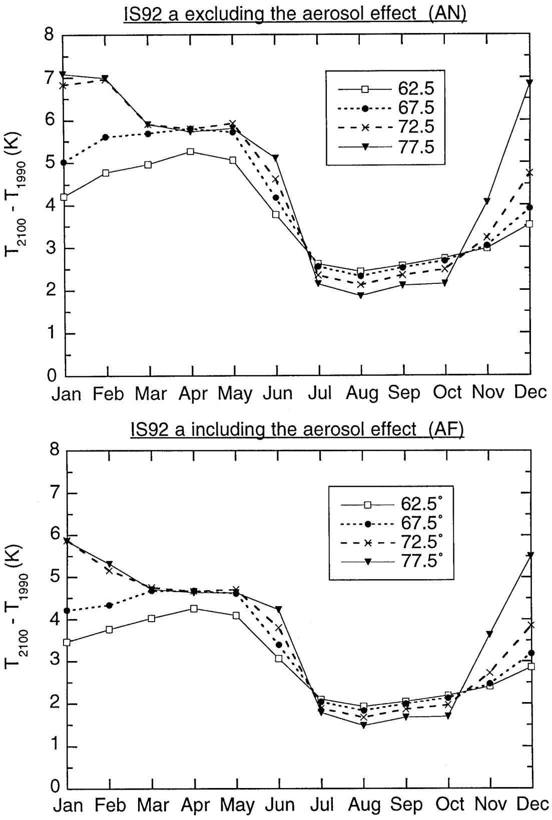

Fig. 5. Seasonal march of input temperature for two scenarios for some selected latitudes, calculated with a 2-D energy balance climate model

5 Sensitivity tests

In this section we describe various experiments designed to estimate the contribution of the Greenland ice-sheet to global sea level. These experiments reveal the sensitivity of the results to: (a) choice of elevation model as input (5.1), (b) neglect of ice dynamics and the choice of mass balance model (5.2), (c) initial state (5.3), (d) neglect of sliding (5.4), (e) constant sensitivity of mass balance to temperature (5.5).

5.1 Choice of elevation model as input

As a start, we investigate to what extent the calculation of ablation depends on the elevation model used (Van de Wal and Ekholm 1996). Most recent work on modelling the mass balance of the Greenland ice-sheet (Huybrechts et al. 1991; Reeh 1991; Van de Wal and Oerlemans 1994) has been based on the digital elevation model presented by Letréguilly et al. (1991) on a grid of 20*20 km resolution (TUD-model). Here we consider two cases, which describe the present-day elevation distribution: the TUD-model and the IA-model (see Sect. 3). For the present-day climate, the two elevation models yield a 20% difference in ablation. This applies to the degree-day model as well as

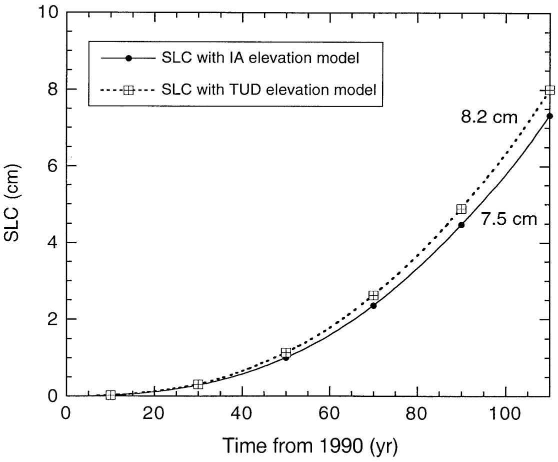

Fig. 6. Sea-level contribution (*SLC*) for the TUD and the *IA*-model elevation distributions for a period of 110 y. The surface elevation is kept constant during the entire period. Calculations were carried out with an energy balance model

to the energy-balance model (Van de Wal and Ekholm 1996).

Figure 6 shows the calculated sea-level contribution (SLC) from the Greenland ice-sheet for a period of 110 y during which surface elevation is kept constant and the temperature perturbation is prescribed according to the AN-scenario (see Fig. 4). This experiment shows that after 110 y there is a difference of about 9% in the calculated sea-level contribution (7.5 cm versus 8.2 cm) between the two elevation models. Clearly, the difference is smaller than the 20% difference found for ablation in the present day climate. This can be understood by the fact that the difference in area-elevation distribution between the two models decreases higher on the ice-sheet. The higher elevations are more important in a perturbation experiment since the ablation increases and the equilibrium line goes up.

Increasing the resolution of the IA-model from 20*20 km to 10*10 km yields virtually identical results, despite the difference in ablation resulting from the contribution of small-scale outlet glaciers. It might however be necessary to use an even higher resolution as indicated by Reeh and Starzer (1996).

5.2 Neglect of ice dynamics and the choice of the mass-balance model

So far we have calculated sea-level changes for a given geometry. For making projections, it would indeed be convenient if changes in the geometry of the ice-sheet could be neglected. Here we discuss the role of the ice dynamics by considering three cases: full dynamic response, static response, and fixed geometry. For the present analysis, the following definitions are used:

Dynamic response. The ice flow is allowed to react to changes in the specific balance or the bedrock response. Hence, the specific balance, ice thickness and bedrock are fully coupled.

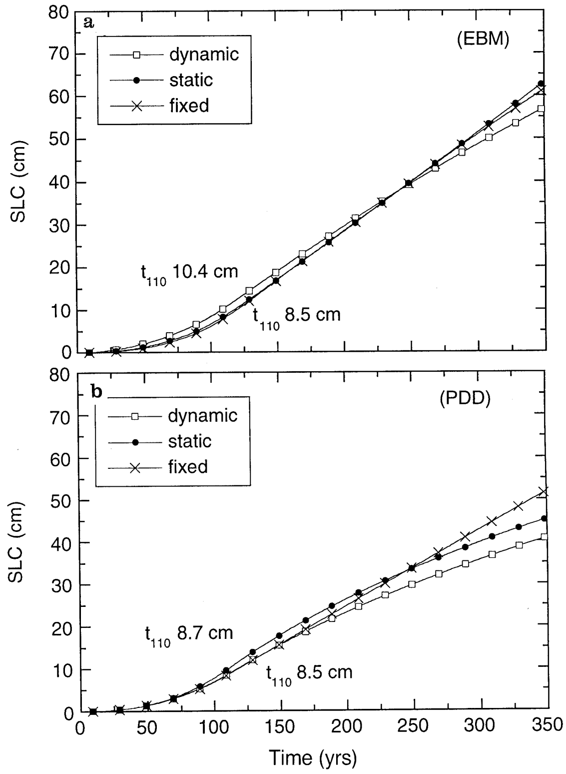

Fig. 7. Sea-level contribution (*SLC*) in case of dynamic, fixed and static response using an energy balance model (*EBM*) and a degree-day model (*PDD*). The forcing scenario is AN. The *text in the figure* refers to the sea-level contribution after 110 y for the dynamic (*upper value*) and fixed-geometry case (*lower value*)

Static response. Changes in ice flow and bedrock are not allowed. The geometry changes only because of the addition or removal of mass at the surface according to the mass-balance perturbation. Note that in this case the feedback of surface elevation on mass balance is still included.

Fixed-geometry response. Changes in volume are calculated from the perturbed specific balance by keeping the ice-sheet geometry fixed. In the IPCC-1990 sea level projections and the energy balance model developed by Van de Wal and Oerlemans (1994) the fixed-geometry response was adopted.

Here, we calculate the response of the ice-sheet to the AN-temperature scenario for these three cases. Figure 7 shows the result for the energy balance model (EBM) and the degree-day model (PDD) as forcing. It should be noted that the perturbation experiments start with a steady-state ice-sheet which is different for the energy balance model ($V_{ref} = 2.73*10^{15}$ m^3) and the degree-day model ($V_{ref} = 3.00*10^{15}$ m^3). Ice dynamics, bedrock response and the additional temperature forcing are formulated identically. It should be mentioned here as well that the degree-day model includes variations in accumulation due to changes in temperature (roughly 5% for 1 K change). However, this does not explain the differences between the EBM-model and the PDD-model. Excluding the coupling between temperature and accumulation leads to a minor change in sea-level contribution for the degree-day model (e.g. 1% after 110 years for the dynamic case). In spite of the increasing sea level temperature, accumulation integrated over the entire ice-sheet does not increase much due to the surface lowering, a result of the increased ablation. The dominating effect in this type of scenario experiments is the increase in ablation. (For a detailed analysis of the differences between the two types of mass balance models for the fixed geometry case the reader is referred to Van de Wal 1996).

The energy balance and degree-day model calculations for the dynamic case indicate that there is a tendency for equilibrium to be restored. After about 250 y the time derivative decreases. As a result, sea-level changes for the fixed-geometry case and the dynamic case deviate strongly from the year 110 onwards (note: from here the forcing is kept constant).

If we look in detail at the response during the first period, we can observe that for both mass-balance formulations the sea-level contribution is larger for the dynamic case than for the fixed-geometry case. After 110 y the energy-balance forcing yields a sea-level contribution of 10.4 cm for the dynamic case and 8.5 cm for the fixed-geometry case. For the degree-day forcing the difference is less pronounced, 8.7 cm versus 8.5 cm (Fig. 7). The reason for the difference between dynamic and fixed-eometry case is that in the former the mass flow to the lower ablation region increases, bringing additional ice to the ablation area. In the fixed-geometry case this does not happen and after a while the ablation area shrinks.

Interpretation of the static case is more complicated. Considering the degree-day model first, after 110 y the sea-level change for the static case is 15% higher than for the dynamic case. Surprisingly, the static response is only 9% higher for a time scale of several hundreds of years. This is due to the fact that further deviation of the static response is limited by the disappearance of ice-covered points at the ice-sheet margin. If a static response would be assumed for several thousands of years, the volume of the ice-sheet would ultimately increase. This is due to the fact that the entire ablation area will disappear and the accumulation will steadily increase, which of course, is physically unrealistic.

If we consider the static approach with the energy-balance method we get another picture. The sensible heat flux in this model depends on the distance to the ice margin: closer to the margin the sensible heat flux increases (higher wind speed and larger surface roughness). Disappearance of ice-covered grid points will therefore make it possible for points initially belonging to the accumulation area to shift to the ablation area. This then means that, also in the long run, the volume of ice-sheet keeps decreasing.

The fixed-geometry approach, however, appears to be justified for a degree-day model on a time scale of a hundred years. But over longer periods it lacks the compensating ice flow of the dynamical response. Therefore it cannot be used for calculations longer than 100 y into the future.

Altogether, it appears that using a static or fixed-geometry approach may lead to erroneous results, depending on the time scale of interest and the type of mass balance model.

5.3 Initial state

If we accept that a fixed-geometry approach is not accurate enough to calculate the contribution of the Greenland ice-sheet to sea-level change, the next step is to consider the dependence of projections on the initial state.

The first question is: should we start with the present-day observed state? Most likely, even without a climate perturbation the model ice-sheet would evolve to a different state. However, because of inaccuracies in observations and model formulation, it would be impossible to judge from this the present imbalance. Thus it seems more straightforward to start with a modelled equilibrium state which resembles the present-day situation, referred to earlier in this study as the reference experiment. This approach has also been used by Huybrechts et al. (1991).

The second question is: to what extent do the projections depend on the chosen initial state? The sensitivity to the choice of initial state is illustrated by three experiments, described briefly. All three runs are performed with inclusion of the geodynamic component and of sliding. The energy-balance model is used to calculate the ablation.

In addition to the steady state of the reference experiment, we calculated two steady-states, one for a climate which is 1 K colder and one for a climate which is 1 K warmer. Starting with these steady-states, the temperature forcing is then the same for all and follows the AN-scenario. By performing such an experiment we think we quantify the range of uncertainty.

Figure 8 shows the results of this experiment. The initial state for the 1 K warmer climate is 7% smaller and for the 1 K colder climate 4% larger than for the reference experiment. These limited deviations from the reference state (Tables 1 and 2), however, lead to considerable differences in calculated sea-level contributions. For a period of 110 y we can observe in Fig. 8b that starting from a 1 K colder climate yields a 50% larger increase than for the reference experiment. On the longer time scale (several hundreds of years) results are less dependent on the initial conditions, as might be expected, but the difference in increase is still about 20%. These results also show that part of the differences in the mass-balance formulation (energy balance or degree-day) described in Fig. 7 may be related to the different steady states for these two experiments ($2.73 \cdot 10^{15}$ m^3 versus $3.00 \cdot 10^{15}$ m^3).

To understand this difference it should be realized that even without an additional forcing volume changes will appear with the 1 K warmer or colder steady-state as initial condition. The ice-sheet will obviously migrate towards the reference state for the present climate. For a 1 K colder climate the response time [The time necessary to reach $V_{response}$; ($V_{response} = V_{-1K} - (V_{-1K} - V_{ref})(1 - 1/e)$] is about 3000 y. Nevertheless 10% of the difference

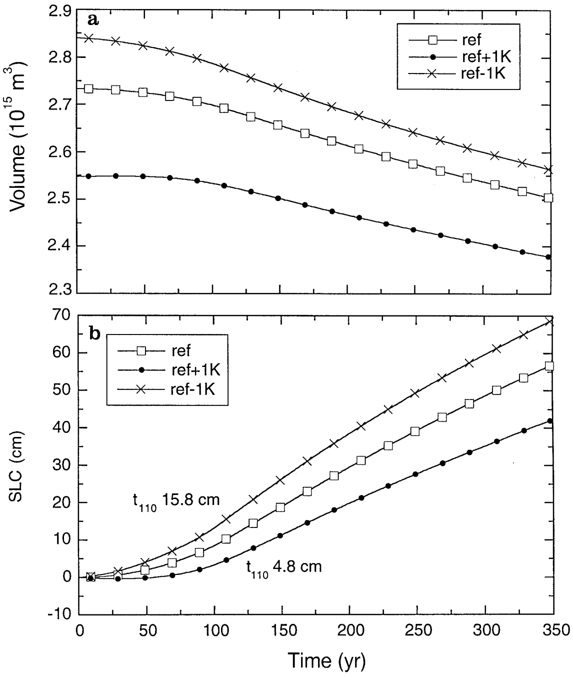

Fig. 8a, b. Illustrating the effect of a different initial state (obtained by varying the temperature by 1 K). **a** Ice volume and **b** sea-level contribution for the AN scenario. The reference run in Fig. 8b is identical to the dynamic case in Fig. 7a

between the two steady states will be reached after only 110 y. This means that approximately 2.7 cm SLC can be expected over a period of hundred years if we start with a reference state which is 1 K colder and without an additional forcing. This is half of the difference in response to the AN-scenario which is respectively 10.4 cm for the reference case and 4.8 cm for the -1 K case. So on one hand there is the tendency to migrate to the reference state for the -1 K case and for the $+1$ K case. On the other hand all three steady-state cases will respond to the additional forcing implied and migrate towards the steady-state belonging to the AN-scenario. As the temperature deviation for this scenario is approximately 4 K (for 65°–70°N) this means a nearly complete disappearance of the ice-sheet. This large forcing implies that the volume change is shortly after the onset independent of the initial steady-state. Observation of cross profiles shows that the differences between the profiles are already negligible after 350 y, whereas they are significantly different for the three initial steady states. In summary one can therefore state that the differences presented in Fig. 7 are entirely a dynamical effect which imply that the results in terms of sea-level change strongly depend on the initial steady-state.

5.4 Neglect of sliding

Another point that is important for the calculation of the response of the ice-sheet to global warming is the formulation of the ice dynamics. Generally, vertical mean ice velocity is considered to be the sum of deformation of ice

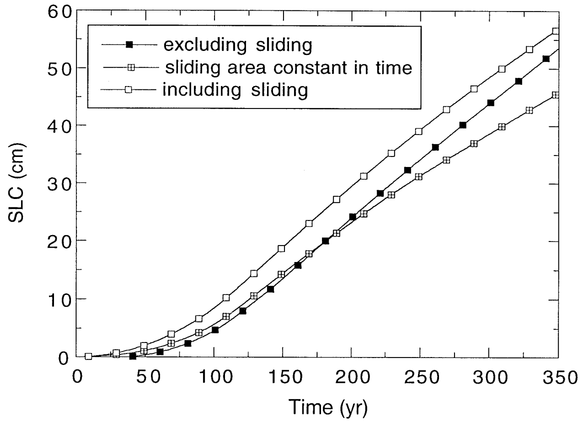

Fig. 9. The effect of sliding for the calculated contribution to sea-level rise (AN scenario). For the run excluding sliding the initial state is different (see text)

and sliding over the bedrock. The latter process is not very well understood and the confidence in model results would be higher if basal sliding could be neglected. To judge whether sliding is important for the dynamic response of the Greenland ice-sheet to climate warming we compare three models runs in Fig. 9.

The run with sliding is the default perturbation experiment (Figs. 7 and 8). As the parametrization of sliding is directly coupled to meltwater production (it is assumed that sliding can only occur in the ablation zone, see Appendix), the sliding area becomes larger in the course of time. It is unlikely that this happens in reality on a 100 y time scale. Thermodynamics are slower, and consequently one cannot expect the glacial drainage system to respond quickly to the size of the ablation area. For this reason we have also conducted a run in which the sliding area was kept fixed. As can be seen in Fig. 9, this produces a different result. As expected, the loss of ice is smaller when the sliding area cannot increase. The difference is about 20%.

Also shown is the result of a run in which no sliding is allowed at all. For a fair comparison, this run has been done with a different initial state. This state has the same ice volume, requiring a larger deformational flow parameter to compensate for the neglect of sliding (as discussed earlier). The shape of the ice-sheet is different (a steeper profile near the margin), which is reflected in a smaller loss of ice for the climate warming experiment. More precisely, the response time of the ice-sheet is larger. It can be seen that after a few hundred years the relative difference with the case with sliding becomes smaller and smaller.

In summary, it can be concluded that sliding has a significant effect on the response of the ice-sheet to climate warming. Neglect of sliding yields a response that is too slow.

5.5 Constant sensitivity

Instead of using detailed energy balance or degree-day calculations, a dynamic response of the ice-sheet and appropriate boundary conditions, one could use a

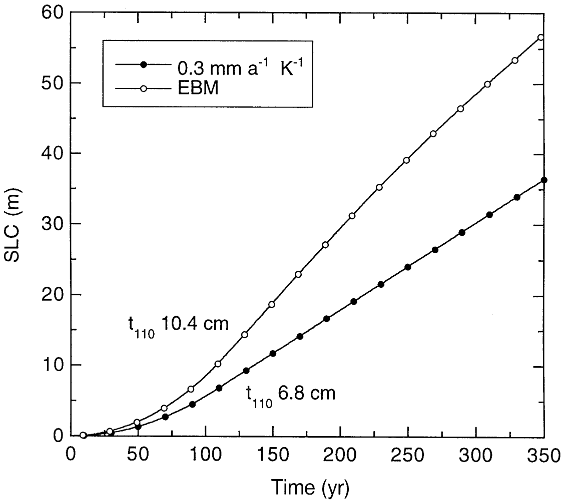

Fig. 10. Sea-level contribution with a constant sensitivity value of 0.3 mm/K y and using output from the energy-balance model as forcing. Both calculations are for a fixed geometry

constant sensitivity multiplied by a temperature perturbation, as was done, for instance, in the 1990 IPCC-report (Warrick and Oerlemans 1990). This constant sensitivity value (expressed in mm sea level change per K y) used by Warrick and Oerlemans (1990) was based upon sensitivity experiments of ablation models for a 1 K perturbation, which is comparable to the sensitivity of the energy balance model and the degree-day model used here. To see whether the use of a constant sensitivity value can be justified, we calculated for this case the contribution to sea-level rise for the AN scenario.

Figure 10 shows the results for the two approaches. In both calculations the geometry of the ice-sheet was fixed ! The difference after 110 y is tremendous. The constant sensitivity predicts a sea level rise of only 6.8 cm, whereas the EBM model predicts 10.4 cm. The reason for this discrepancy is the increasing sensitivity incorporated in the EBM model. Van de Wal (1996) showed that the sensitivity of the energy balance model increased from 0.31 mm/K y for a 1 K perturbation to 0.58 mm/K y for a 4 K perturbation. The increasing sensitivity can be observed in the degree-day model as well.

The conclusion is that the use of a constant sensitivity value is not justified if perturbations are larger than 1 K.

6 Climate change experiments

Before we apply the IPCC scenarios (Sect. 7), we consider three other aspects that are important for climate change experiments. Respectively, we will consider the choice of the reference year, the seasonal cycle, and natural climate variability.

6.1 The choice of the reference year

It could be argued that it is necessary to capture lag effects in the climate system (Warrick et al. 1996). For this reason,

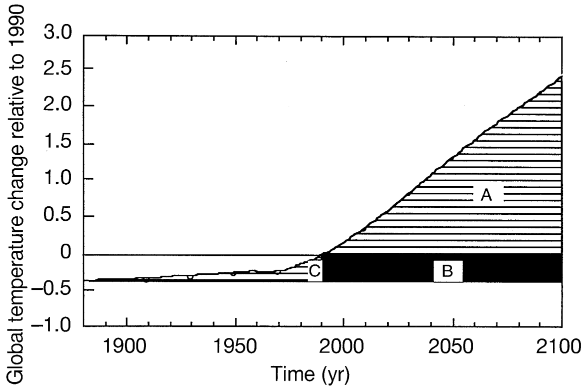

Fig. 11. Sea level change for constant sensitivity (S) for the AN-scenario over the period 1990–2100

some of the calculations on sea-level rise presented by IPCC (Warrick et al. 1996) start in 1880. If one is interested in sea-level rise over the period 1990–2100, some objections against this approach can be made, however. We illustrate this in the following example for the AN-scenario, see Fig. 11.

Starting the time integration in 1880 means that the contribution to sea-level rise since 1880, assuming constant mass-balance sensitivity, is the sum of the areas A, B and C multiplied by the sensitivity (denoted by $S1880$). If the period under study is 1990–2100, area C must be subtracted. Since perturbations are expressed relative to 1880, we need to know the sensitivity of the Greenland ice-sheet in 1880, but this is unknown. Because it is unknown it is assumed that the sensitivity to be equal to that of the present-day ($S_{1880} = S_{1990}$). But model results upon which the sensitivity value of 0.3 mm/K y is based refer to a simulation of the present-day situation, which is not necessarily identical to the 1880 situation. This means that the appropriate sea-level rise, for the period 1990–2100, is area A times the sensitivity in 1990. The difference between the two approaches is area B.

A calculation following this procedure shows that, for the period 1990–2100 with the AN-scenario, the IPCC result overestimates the contribution to global sea-level rise by about 30% for the period 1990–2100 (5.4 cm for the IPCC estimate, 4.1 cm when starting in 1990). We note that the increasing sensitivity for larger temperature perturbations adds an additional error because the adopted reference temperature in 1880 is lower than in 1990.

6.2 The role of the seasonal cycle

So far, we have used monthly mean temperature perturbations to evaluate the contribution of the Greenland ice-sheet to sea-level rise. We did this because the temperature increase is not constant through the year. Predicted summer warming is less than predicted winter warming (see Fig. 5). Most melting occurs in summer, so a smaller temperature change in summer reduces the projected ablation rates. We have repeated the calculations for the AN scenario with the mean annual temperature as forcing. This indeed results in increased loss of ice, although the effect is not dramatic (10% after 110 y).

6.3 Natural climate variability

Before results for the IPCC scenarios are summarized, it is worth considering the effect of climate variability. For this purpose we have forced the model by a random series of annual mean temperature and precipitation perturbations, taken in a uniform way over the ice-sheet. The strength of this forcing (standard deviation) is 0.66 K for temperature and 12% for precipitation. These values are based on a compilation of annual mean temperatures at Greenland stations over the period 1870–1990, and on accumulation records from ice cores (Dibb 1992). The mean random perturbation is zero for temperature as well as for precipitation.

If the additional random forcing is imposed on the model, hardly any differences on the contribution to sea-level change can be observed. The reason is that the predicted temperature forcing after 100 y is already 3–4 K, which obviously has a larger impact than a random temperature forcing of 0.66 K. Nevertheless, the experiment provides some confidence in the use of monthly mean temperature perturbations and indicates the limited importance of variability. Variability will only be important if its strength is of the same order of magnitude as the secular trend in the forcing.

7 Results for IPCC-1996 scenarios

Finally, we imposed the IPCC scenarios described in Sect 4 as forcing to the model. Although not all IPCC scenarios published in the IPCC reports have been used, we have included the extreme ones to see the full range of possible Greenland contributions to sea-level rise.

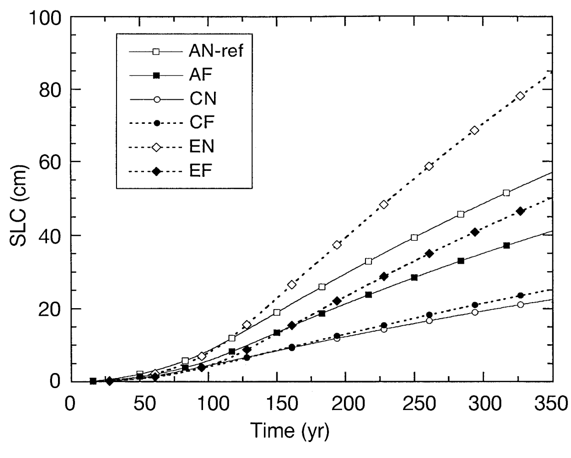

Fig. 12. Greenland contribution to sea-level change obtained with the full model for the various climate scenarios. Included are bedrock adjustment, sliding and the energy-balance model to calculate ablation. Runs start from a modelled steady state. Results for the AN-scenario are included in Fig. 9 (the curve "including sliding") and Figs. 7a and 8b

The forcing is formulated as monthly temperature perturbations relative to 1990. The model version for these runs has isostatic bedrock response, sliding, and the energy-balance model to calculate ablation. If the A-scenario for equivalent greenhouse forcing is considered most likely, the best estimate of the contribution of the Greenland ice-sheet to sea-level rise is 7.0 cm in the year 2100 (AF scenario) or 10.4 for the AN-scenario (Fig. 12). Associated with the different climate scenarios used we observe a range of predictions from 5–11 cm for the year 2100 and 20–85 cm for the year 2340.

8 Discussion

This study presents results for the short-term response of the Greenland ice-sheet to enhanced greenhouse warming. The estimated contribution to global sea level is 10.4 cm in 2100 for the AN-scenario. This figure is based on calculations starting from a dynamic equilibrium of a two-dimensional ice-sheet model, including sliding and a dynamic bed response. Ablation is calculated with an energy balance model. However, several mechanisms influence this result considerably. Table 3 presents an overview of the experiments described in this study. Table 3 shows the most important results of this work, described by the information in the first six columns of the table. The last column refers to the figure in which these results have been presented.

One of the results presented in Table 3 indicates that the contribution of the Greenland ice-sheet is actually larger than the value of 10.4 cm presented in the IPCC-96 report. Transient effects due to the slowly increasing temperature in the past may increase the response by a similar amount. This means that future modelling work should concentrate on historical simulations. Table 3 also shows that for a fixed geometry results depend significantly on the resolution of the model. This is probably the case for the dynamic response as well, but this cannot yet be investigated because at present ice thickness data are insufficient.

From all the experiments presented here it is clear that one should be very careful in making simplifications. For instance it is necessary to take the increasing sensitivity to larger perturbations into account. This does not mean that complicated ablation models are necessary for all purposes. But at least it is advisable to use the sensitivity derived from these models as a function of the temperature perturbation. Since the sensitivity of the ice-sheet to temperature perturbation is based upon a simulation of the present-day ice-sheet, we cannot take climate lag effects into account in a simple manner. The only way to do this would be by using transient dynamic models. These, however, are difficult to validate due to lack of historical data.

The climate experiments show that it hardly matters whether yearly temperature scenario or monthly mean values are used. The results differ by only 10%. Climate variability is also not very important either, at least on the time scale analyzed and given the magnitude of the perturbations, but care should be taken with the choice of the reference year.

Table 3. An overview of the experiments presented in this study

Response	Mass balance	Intial volume ($*10^{15}$ m^3)	Dynamic equilibrium	Sliding	Resolution (km)	SLC $t = 110$ (cm)	SLC $t = 350$ (cm)	Figure
Dynamic	EBM	2.73	REF[a]	Yes[b]	20	10.4	57.0	7b,8b,9,12
Fixed	EBM	2.73	IA[c]	Yes[b]	20	7.5	–	6
Fixed	EBM	2.82	IA[c]	Yes[b]	10	7.5	–	
Fixed	EBM	2.83	TUD[c]	Yes[b]	20	8.2	–	6
Fixed	EBM	2.73	REF[a]	Yes[b]	20	8.5	63.0	7a
Static	EBM	2.73	REF[a]	Yes[b]	20	8.0	61.4	7a
Dynamic	PDD	3.00	Yes[b]	Yes[b]	20	8.7	40.8	7b
Fixed	PDD	3.00	Yes[b]	Yes[b]	20	8.5	51.8	7b
Static	PDD	3.00	Yes[b]	Yes[b]	20	9.8	45.2	7b
Dynamic	EBM	2.55	Yes[b]	Yes[b]	20	4.8	42.2	8b
Dynamic	EBM	2.84	Yes[b]	Yes[b]	20	15.8	68.9	8b
Dynamic	EBM	2.76	Yes[b]	No	20	6.0	53.6	9

The column dynamic equilibrium contains information on whether the initial state is a dynamic equilibrium or an observed elevation model
[a]REF means the reference equilibrium state described earlier in this study
[b]Yes, means a dynamic equilibrium not equal to the reference case
[c]IA and TUD are the non-equilibrium states of the present-day observations

A comparison of the results from the section climate change experiments and sensitivity experiments indicate that the variability in the response on a time scale of a hundred years is partly a consequence of the uncertainty in the climate scenarios but depends more on the actual formulation of the applied model. On a time scale of a few hundred years the variability is dominated by the variability in the climate scenarios, (Table 3 and Fig. 12).

Appendix A: description of the model

The ice-sheet model treats ice flow by solving the equations on a two-dimensional grid with a grid-point distance of 20 km in the horizontal plane. The ice dynamics are described in a single vertically averaged layer (Mahaffy 1976; Cadee 1992), where ice velocity is determined by the local driving stress (τ) only. This means that longitudinal deviationary stresses are disregarded. No thermodynamics are included in the model. It is time-dependent and also includes the response of the underlying bedrock to changing ice load. The surface mass balance and ice thickness are entirely coupled. The model equations are

$$\frac{\partial H}{\partial t} = -\nabla(\vec{v}H) + M \qquad \text{A.1}$$

In Eq. (A.1) H is ice thickness, $\vec{v}$ the depth-averaged horizontal velocity field (in m/y), M the mass balance (in m water equivalents/y) and t time (in y). The vertical mean ice velocity $\vec{v}$ consists of two parts: one associated with internal deformation (first term in A.2) and one associated with basal sliding (second term in A.2). Both parts increase with the third power of the driving stress.

$$\vec{v} = fH\tau^3 + \frac{f^* \tau^3}{N-P} \qquad \text{A.2}$$

The flow parameters f and f^* are set to $4.0*10^{-17}$ $m^6N^{-3}y^{-1}$ and $2.0*10^{-10}$ $m^5N^{-2}y^{-1}$, respectively. These parameters must be considered as tuning parameters of the model and are obtained by comparing predicted ice thickness and observed ice thickness. In case of the no-sliding experiment f is $14.0*10^{-17}$ $m^6N^{-3}y^{-1}$ and f^* zero. From the definition of Eq. (A.2) it follows that sliding is inversely proportional to normal load (N) minus basal water pressure (P). Variations in basal water pressure are not allowed in this study. It is simply assumed that $N - P = 0.8*N$. Sliding is restricted to areas where surface melting occurs.

The equation for the driving stress (τ) reads:

$$\tau = -\rho_i g H \frac{\partial h_s}{\partial x} \qquad \text{A.3}$$

Here ρ_i is the ice density, g gravitational acceleration and h_s surface elevation which is the sum of bedrock elevation (h_b) and ice thickness.

As stated before, the model also takes into account bedrock adjustment in response to a changing ice load. In the experiments an isostatic lithosphere, ($w = \rho_i/\rho_m*H$) has been used. It could be argued that an elastic plate is more appropriate. The difference between pure isostatic equilibrium and an elastic plate is generally small except near the margins of an ice-sheet. Because of the short time scale considered in this study, this simplification is probably not important for volume changes.

In order to calculate the time evolution, we use a linear viscous asthenosphere model (channel model). This yields the diffusion equation:

$$\frac{\partial h_b}{\partial t} = D_a \nabla^2 (h_b - h_0 + w) \qquad \text{A.4}$$

where h_0 is the undisturbed bed elevation if the ice sheet is removed and D_a a diffusion coefficient ($5.0*10^7$ m^2 y^{-1}).

The only remaining unknown quantity in the set of equations described so far is the mass balance (M). Two types of mass-balance models are considered. First we describe the energy balance approach (EBM) and secondly the degree-day approach (PDD). Both methods yield the net mass balance (M) at a specific point, as used in equation A.1.

The energy balance method is identical to the model used by Van de Wal and Oerlemans (1994) and only the main characteristics will be described here. In this model ablation is calculated on an irregular grid with a minimum spacing of 20 km. The ablation at the other points in the 20 km grid are linearly interpolated from the first group of points. In this version the energy balance is calculated with a time step of only 40 min (to resolve the daily cycle). Input data for the EBM calculations are the surface topography, cloudiness, surface temperature and accumulation. For the surface temperature distribution the compilation of Ohmura (1987) has been used. The annual accumulation is taken from Ohmura and Reeh (1991). It should be noted that for the EBM calculation the annual accumulation is independent of the temperature; this is not the case in the PDD calculations. Cloudiness varies with latitude and with the distance from the margin of the ice sheet, which might migrate during an experiment. Surface topography varies with ice thickness and bedrock adjustment. The surface temperature field itself is parametrized as a function of latitude and surface topography and thus interacts freely with changes in ice dynamics.

An important point in the model formulation is that the albedo is a function of snow depth, ablation, amount of meltwater at the surface and the type of surface. Due to this albedo formulation the EBM model responds nonlinearly to changing climatic input.

The degree-day approach is identical to the formulation used by Huybrechts et al. (1991). This model calculates the ablation in terms of mean annual air temperature and summer air temperature, and is based on work by Ohmura (1987). Input for the PDD calculations are the surface topography, surface temperature and accumulation. The surface temperature and accumulation used in the EBM version and PDD versions are identical. As stated already, the accumulation distribution is only considered to be temperature-dependent in the degree-day version, which is in accordance with the work of Huybrechts et al. (1991) and Van de Wal and Oerlemans (1994).

Boundary conditions

Model calculations start from the present state as presented by Letréguilly et al. (1991) which is not necessarily in equilibrium with the equations A.1-A.5. The model is integrated 15 ky forwards in time to obtain the reference steady state. Bed topography, ice thickness and the latitudinal coordinates are the main input fields. The data sets used here were composed by Letréguilly et al. (1991). In the model the ice-sheet is limited to the present coastline. The ocean is considered as an infinite sink of ice. Formation of ice shelves and details of calving are not considered. Once the ice reaches the ocean, ice thickness is immediately set to zero. The reason for doing this is the small scale of outlet glaciers in combination with the fact that in this study the main interest is focused on the short time scale.

Numerical details

The calculation are performed on a horizontal grid with spacing of 20 km (11 703 points in total). Deflection is calculated at every second grid point in order to save computer time. The finite difference equations describing changes in ice thickness (A.3) and bedrock (A.5) are solved numerically by the alternating direction implicit method. For the calculation of steady-states model time steps are 4 y for the changes in ice thickness and 40 y for the more slowly varying change in bedrock. Once a steady-state is calculated and perturbations experiments are started all time steps are 1 year. One-year time steps are used because the external perturbations of the mass balance are given on an annual basis and time integration is relatively short in this study (350 y).

References

Cadee M (1992) Numerical modelling of the Greenland ice sheet, application of a two-dimensional ice flow model (in Dutch). IMAU Int Rep V92–10.

De Wolde JR, Bintanja R, Oerlemans J (1995) On the thermal expansion over the last hundred years. J Clim (in press)

Dibb JE (1992) The accumulation of ^{210}Pb at Summit, Greenland since 1855. Tellus 44b: 72–79

Ekholm S (1996) A full coverage, high resolution, topographic model of Greenland, computed from a variety of digital elevation data. J Geophys Res 101:21 961–21 972

Huybrechts P (1994) The present evolution of the Greenland ice-sheet: an assessment by modelling. Global Planet Change 9: 39–51

Huybrechts P, Oerlemans J (1990) Response of the Antarctic ice-sheet to future greenhouse warming. Clim Dyn 5: 93–102

Huybrechts P, Letréguilly A, Reeh N (1991) The Greenland ice-sheet and greenhouse warming. Paleogeogr, Palaeoclim, Paleoecol (Global Planet Change Sect), 89 (4): 399–412

Kattenberg A, Giorgi F, Grassl H, Meehl GA, Mitchell JFB, Stouffer RJ, Tokioka T, Weaver AJ Wigley TML (1996) Climate models-projections of future climate. In: Houghton JT, Meiro Filho LG, Callander BA, Harris N, Kattenberg A and Maskell K (eds) The science of climate change-Climate change 1995. Cambridge University Press, Cambridge pp. 285–357

Letréguilly A, Huybrechts P, Reeh N (1991) Steady-state characteristics of the Greenland Ice Sheet under different climates. J Glaciol, 37 (125): 149–157

Mahaffy MW (1976) A three-dimensional numerical model of ice-sheets: tests on the Barnes Ice Cap, Northwest Territories. J Geophys Res 81: 1059–1066

Oerlemans J (1982) Response of the Antarctic Ice-Sheet to a climatic warming: a model study. J Climatol 2: 1–11

Oerlemans (1989) A projection of future sea level. Clim Change 15: 151–174

Ohmura A (1987) New temperature distribution maps for Greenland. Z Gletscherkd Glazialgeol 23 (1): 1–45

Ohmura A, Reeh N (1991) New precipitation and accumulation maps for Greenland. J Glaciol 37 (125): 140–148

Reeh N (1991) Parametrization of melt rate and surface temperature on the Greenland Ice-Sheet. *Polarforschung* **59**(3): 113–128.

Reeh N, Starzer W (1996) Spatial resolution of ice-sheet topography: influence on Greenland mass-balance modelling, GGU rapport 1996/53: 85–94.

Robin G de Q (1986) Changing the sea level. In: Bolin B, Döös BR, Jäger J, Warrick RA (eds) The greenhouse effect. climatic change and ecosystems. Scope 29, John Wiley, New York: pp. 323–359

Van de Wal RSW (1996) Mass-balance modelling of the Greenland ice-sheet: a comparison of an energy balance and a degree-day model. Ann Glaciol 23: 36–45

Van de Wal RSW, Ekholm S (1996). On elevation models as input for mass balance calculations of the Greenland ice-sheet. Ann Glaciol 23: 181–186
Van de Wal RSW, Oerlemans J (1994) An energy balance model for the Greenland Ice-Sheet. Global Planet Change 9: 115–131
Warrick RA, Oerlemans J (1990) Sea level rise. In: Houghton JT, Jenkins GJ, Ephraums JJ (eds), Climate Change, The IPCC Scientific Assessment. Cambridge University. Press Houghton JT, Jenkins GJ Ephraums JJ (eds): 261–281
Warrick RA, Le Provost C, Meier MF, Oerlemans J, Woodworth PL (1996) Changes in sea level. In: Houghton JT, Meiro Filho LG, Callander BA, Harris N, Kattenberg A, Maskell K (eds), climate change 1995 - The science of climate change. Cambridge University Press Cambridge, pp 359–405